

# Geometric design using space curves with rational rotation-minimizing frames

Rida T. Farouki<sup>1</sup>, Carlotta Giannelli<sup>2</sup>, and Alessandra Sestini<sup>3</sup>

<sup>1</sup> Department of Mechanical and Aeronautical Engineering,  
University of California, Davis, CA 95616, USA

<sup>2</sup> Dipartimento di Sistemi e Informatica, Università degli Studi di Firenze,  
Viale Morgagni 65, 50134 Firenze, ITALY

<sup>3</sup> Dipartimento di Matematica “Ulisse Dini,” Università degli Studi di Firenze,  
Viale Morgagni 67a, 50134 Firenze, ITALY  
e-mail: farouki@ucdavis.edu, giannelli@dsi.unifi.it,  
alessandra.sestini@unifi.it

**Abstract.** A rotation-minimizing adapted frame  $(\mathbf{f}_1(t), \mathbf{f}_2(t), \mathbf{f}_3(t))$  on a given space curve  $\mathbf{r}(t)$  is characterized by the fact that the frame vector  $\mathbf{f}_1$  coincides with the tangent  $\mathbf{t} = \mathbf{r}' / |\mathbf{r}'|$ , while the frame angular velocity  $\boldsymbol{\omega}$  maintains a zero component along it, i.e.,  $\boldsymbol{\omega} \cdot \mathbf{t} \equiv 0$ . Such frames are useful in constructing swept surfaces and specifying the orientation of a rigid body moving along a given spatial path. Recently, the existence of quintic polynomial curves that have *rational* rotation-minimizing frames (quintic RRMF curves) has been demonstrated. These RRMF curves are necessarily Pythagorean-hodograph (PH) space curves, satisfying certain non-linear constraints among the complex coefficients of the Hopf map representation for spatial PH curves. Preliminary results on the design of quintic RRMF curves by the interpolation of  $G^1$  spatial Hermite data are presented in this paper. This problem involves solving a non-linear system of equations in six complex unknowns. The solution is obtained by a semi-numerical scheme, in which the problem is reduced to computing positive real roots of a certain univariate polynomial. The quintic RRMF  $G^1$  Hermite interpolants possess one residual angular degree of freedom, which can strongly influence the curve shape. Computed examples are included to illustrate the method and the resulting quintic RRMF curves.

**Key words:** Pythagorean-hodograph space curves; rational rotation-minimizing frames; Hermite interpolation; Hopf map representation.

## 1 Introduction

In applications such as computer animation, motion control, and swept surface constructions, it is often necessary to specify the variation of an orthonormal frame along a curved path, that describes the orientation of a rigid body as it traverses this path. In typical cases, one frame vector is prescribed *a priori* (e.g., the unit tangent vector to the path, or the unit polar vector from a fixed origin to each point of the path) and only one degree of freedom remains, associated

with the orientation of the two frame vectors in the plane orthogonal to this prescribed vector at each curve point. Frames that incorporate the unit tangent and unit polar vector as one component are known as *adapted* and *directed* curve frames, respectively [7]. An infinitude of such frames exists on any given space curve, but among them the *rotation–minimizing frames* (or RMFs) are of special interest. The distinctive property of RMFs is that their angular velocity always maintains a zero component in the direction of the prescribed frame vector.

The focus of this paper is on rotation–minimizing adapted frames — and, in particular, the construction of curves with *rational* rotation–minimizing frames (or RRMF curves). Specifically, the problem of constructing such curves through interpolation of  $G^1$  Hermite data (end points and tangents) is addressed. The rational dependence of RMFs on the curve parameter is desirable on account of its exactitude, its compatibility with native CAD system representations, and the efficient subsequent computations it facilitates. The existence of non–degenerate quintic space curves with rational RMFs (or quintic RRMF curves) has recently been demonstrated in [9]. Such curves are necessarily Pythagorean–hodograph (PH) space curves, and the basis for the procedure described herein is the system of constraints [9] on the complex coefficients in the Hopf map representation of spatial PH curves, that characterizes RRMF curves.

The problem of Hermite interpolation by spatial PH curves typically admits a multiplicity of formal solutions. For example, the construction of  $C^1$  spatial PH quintic Hermite interpolants incurs selection of two residual angular parameters [6, 8, 16]. Since spatial PH quintics must satisfy three scalar constraints in order to be RRMF curves, relaxing from  $C^1$  to  $G^1$  Hermite data results in a net loss of one residual degree of freedom — i.e., the quintic RRMF interpolants to spatial  $G^1$  Hermite data comprise a *one–parameter family* of solutions.

The plan for this paper is as follows. After briefly reviewing the conditions for a PH space curve to have an RRMF in Section 2, the problem of  $G^1$  Hermite interpolation using RRMF quintics is formulated in Section 3. A procedure for solving this problem is then described in Section 4, and a selection of computed examples is presented in Section 5. Finally, Section 6 summarizes the key results of this paper and makes some concluding remarks.

## 2 Rational RMFs on polynomial space curves

An *adapted* frame on a regular parametric space curve  $\mathbf{r}(t)$  is an orthonormal basis  $(\mathbf{f}_1(t), \mathbf{f}_2(t), \mathbf{f}_3(t))$  for  $\mathbb{R}^3$  such that  $\mathbf{f}_1$  coincides with the unit tangent  $\mathbf{t} = \mathbf{r}' / |\mathbf{r}'|$ . The variation of such a frame may be characterized by its angular velocity  $\boldsymbol{\omega}(t)$ , such that

$$\frac{d\mathbf{f}_1}{dt} = \sigma \boldsymbol{\omega} \times \mathbf{f}_1, \quad \frac{d\mathbf{f}_2}{dt} = \sigma \boldsymbol{\omega} \times \mathbf{f}_2, \quad \frac{d\mathbf{f}_3}{dt} = \sigma \boldsymbol{\omega} \times \mathbf{f}_3,$$

$\sigma(t) = |\mathbf{r}'(t)|$  being the parametric speed of the curve. Among all adapted frames on a given space curve, the *rotation–minimizing frames* (RMFs) exhibit the least possible magnitude  $|\boldsymbol{\omega}(t)|$  of the frame angular velocity [1, 12, 15]. An RMF may

be characterized by the property that its angular velocity maintains a vanishing component in the direction of  $\mathbf{f}_1 = \mathbf{t}$ , i.e.,  $\boldsymbol{\omega} \cdot \mathbf{t} \equiv 0$ , and hence the instantaneous rate of rotation of  $\mathbf{f}_2$  and  $\mathbf{f}_3$  about  $\mathbf{f}_1$  is always zero.

In general, the RMFs of polynomial or rational curves do not admit rational dependence on the curve parameter, and this fact has prompted several authors to propose schemes for peicewise-rational RMF approximations [11, 14, 17, 18]. Clearly, a polynomial space curve  $\mathbf{r}(t) = (x(t), y(t), z(t))$  that admits a rational RMF — i.e., an *RRMF curve* — must have a *rational* unit tangent vector, and it must therefore be a Pythagorean-hodograph (PH) curve [5], whose derivative or hodograph  $\mathbf{r}'(t) = (x'(t), y'(t), z'(t))$  satisfies

$$|\mathbf{r}'(t)|^2 = x'^2(t) + y'^2(t) + z'^2(t) = \sigma^2(t) \quad (1)$$

for some polynomial  $\sigma(t)$ . Two useful (equivalent) representations for spatial PH curves, introduced in [3], are based on the algebra of quaternions  $\mathbb{H}$  and the Hopf map, expressed in terms of complex number pairs  $\mathbb{C} \times \mathbb{C}$ .

Exact RMFs can be computed for any spatial PH curve [4], but in general they incur transcendental functions. The RRMF curves form a proper subset of all spatial PH curves. Using the quaternion model, it was shown in [13] that no RRMF cubics exist, except the degenerate cases of linear or planar curves. Subsequently, the existence of non-degenerate RRMF quintics was demonstrated in [9], using the Hopf map model, and conditions on the complex coefficients in this model were introduced, that identify a spatial PH quintic as an RRMF curve. The Hopf map  $H : \mathbb{C} \times \mathbb{C} \rightarrow \mathbb{R}^3$  specifies a spatial Pythagorean hodograph in terms of two complex polynomials  $\boldsymbol{\alpha}(t) = u(t) + i v(t)$ ,  $\boldsymbol{\beta}(t) = q(t) + i p(t)$  as

$$\mathbf{r}'(t) = H(\boldsymbol{\alpha}(t), \boldsymbol{\beta}(t)), \quad (2)$$

where

$$H(\boldsymbol{\alpha}(t), \boldsymbol{\beta}(t)) = (|\boldsymbol{\alpha}(t)|^2 - |\boldsymbol{\beta}(t)|^2, 2 \operatorname{Re}(\boldsymbol{\alpha}(t)\overline{\boldsymbol{\beta}}(t)), 2 \operatorname{Im}(\boldsymbol{\alpha}(t)\overline{\boldsymbol{\beta}}(t))). \quad (3)$$

In order to define an RRMF curve, the complex polynomials  $\boldsymbol{\alpha}(t)$ ,  $\boldsymbol{\beta}(t)$  in (3) must satisfy [9, 13] the condition

$$\frac{\overline{\boldsymbol{\alpha}}\boldsymbol{\alpha}' - \boldsymbol{\alpha}'\boldsymbol{\alpha} + \overline{\boldsymbol{\beta}}\boldsymbol{\beta}' - \boldsymbol{\beta}'\boldsymbol{\beta}}{\overline{\boldsymbol{\alpha}}\boldsymbol{\alpha} + \overline{\boldsymbol{\beta}}\boldsymbol{\beta}} = \frac{\overline{\mathbf{w}}\mathbf{w}' - \mathbf{w}'\mathbf{w}}{\overline{\mathbf{w}}\mathbf{w}}, \quad (4)$$

where  $\mathbf{w}(t) = a(t) + i b(t)$  is a complex polynomial with  $\gcd(a(t), b(t)) = \text{constant}$ . As noted in [9], when  $\mathbf{w}(t)$  is either a real polynomial or a constant, the condition (4) becomes

$$\overline{\boldsymbol{\alpha}}\boldsymbol{\alpha}' - \boldsymbol{\alpha}'\boldsymbol{\alpha} + \overline{\boldsymbol{\beta}}\boldsymbol{\beta}' - \boldsymbol{\beta}'\boldsymbol{\beta} = 0.$$

This circumstance identifies coincidence of the RMF with the *Euler-Rodrigues frame* (ERF) — a rational adapted frame defined [2] for any spatial PH curve,

that may be expressed in terms of the Hopf map model as

$$\begin{aligned}\mathbf{e}_1(t) &= \frac{(|\boldsymbol{\alpha}|^2 - |\boldsymbol{\beta}|^2, 2 \operatorname{Re}(\boldsymbol{\alpha}\bar{\boldsymbol{\beta}}), 2 \operatorname{Im}(\boldsymbol{\alpha}\bar{\boldsymbol{\beta}}))}{|\boldsymbol{\alpha}|^2 + |\boldsymbol{\beta}|^2}, \\ \mathbf{e}_2(t) &= \frac{(-2 \operatorname{Re}(\boldsymbol{\alpha}\boldsymbol{\beta}), \operatorname{Re}(\boldsymbol{\alpha}^2 - \boldsymbol{\beta}^2), \operatorname{Im}(\boldsymbol{\alpha}^2 + \boldsymbol{\beta}^2))}{|\boldsymbol{\alpha}|^2 + |\boldsymbol{\beta}|^2}, \\ \mathbf{e}_3(t) &= \frac{(2 \operatorname{Im}(\boldsymbol{\alpha}\boldsymbol{\beta}), -\operatorname{Im}(\boldsymbol{\alpha}^2 - \boldsymbol{\beta}^2), \operatorname{Re}(\boldsymbol{\alpha}^2 + \boldsymbol{\beta}^2))}{|\boldsymbol{\alpha}|^2 + |\boldsymbol{\beta}|^2}.\end{aligned}\quad (5)$$

It was shown in [2] that the ERF is not rotation-minimizing for any non-planar RRMF cubic or quintic. Nevertheless, the ERF serves as a useful rational adapted “reference” frame in the problem of identifying RRMF curves.

To define an RRMF quintic, we employ complex quadratic polynomials

$$\begin{aligned}\boldsymbol{\alpha}(t) &= \boldsymbol{\alpha}_0(1-t)^2 + \boldsymbol{\alpha}_1 2(1-t)t + \boldsymbol{\alpha}_2 t^2, \\ \boldsymbol{\beta}(t) &= \boldsymbol{\beta}_0(1-t)^2 + \boldsymbol{\beta}_1 2(1-t)t + \boldsymbol{\beta}_2 t^2,\end{aligned}\quad (6)$$

in (3), where  $\boldsymbol{\alpha}_k, \boldsymbol{\beta}_k \in \mathbb{C}$  for  $k = 0, 1, 2$ . The constraints on these six coefficients that identify non-degenerate RRMF quintics are

$$(|\boldsymbol{\alpha}_0|^2 + |\boldsymbol{\beta}_0|^2)|\bar{\boldsymbol{\alpha}}_1\boldsymbol{\alpha}_2 + \bar{\boldsymbol{\beta}}_1\boldsymbol{\beta}_2|^2 = (|\boldsymbol{\alpha}_2|^2 + |\boldsymbol{\beta}_2|^2)|\boldsymbol{\alpha}_0\bar{\boldsymbol{\alpha}}_1 + \boldsymbol{\beta}_0\bar{\boldsymbol{\beta}}_1|^2, \quad (7)$$

$$(|\boldsymbol{\alpha}_0|^2 + |\boldsymbol{\beta}_0|^2)(\boldsymbol{\alpha}_0\boldsymbol{\beta}_2 - \boldsymbol{\alpha}_2\boldsymbol{\beta}_0) = 2(\boldsymbol{\alpha}_0\bar{\boldsymbol{\alpha}}_1 + \boldsymbol{\beta}_0\bar{\boldsymbol{\beta}}_1)(\boldsymbol{\alpha}_0\boldsymbol{\beta}_1 - \boldsymbol{\alpha}_1\boldsymbol{\beta}_0). \quad (8)$$

It has been shown in [9] that these are necessary and sufficient for the existence of a quadratic complex polynomial  $\mathbf{w}(t)$  such that (4) is satisfied. Since (7) and (8) are constraints on *real* and *complex* values, respectively, they amount to *three* scalar constraints on the coefficients of the polynomials  $\boldsymbol{\alpha}(t)$  and  $\boldsymbol{\beta}(t)$ .

Once the coefficients of the two quadratic polynomials  $\boldsymbol{\alpha}(t)$ ,  $\boldsymbol{\beta}(t)$  satisfying (7) and (8) are known, the coefficients of the polynomial

$$\mathbf{w}(t) = \mathbf{w}_0(1-t)^2 + \mathbf{w}_1 2(1-t)t + \mathbf{w}_2 t^2$$

in (4) are given [9] in terms of them by

$$\mathbf{w}_0 = 1, \quad \mathbf{w}_1 = \frac{\bar{\boldsymbol{\alpha}}_0\boldsymbol{\alpha}_1 + \bar{\boldsymbol{\beta}}_0\boldsymbol{\beta}_1}{|\boldsymbol{\alpha}_0|^2 + |\boldsymbol{\beta}_0|^2}, \quad \mathbf{w}_2 = \frac{\bar{\boldsymbol{\alpha}}_1\boldsymbol{\alpha}_2 + \bar{\boldsymbol{\beta}}_1\boldsymbol{\beta}_2}{\boldsymbol{\alpha}_0\bar{\boldsymbol{\alpha}}_1 + \boldsymbol{\beta}_0\bar{\boldsymbol{\beta}}_1}.$$

The rational RMF  $(\mathbf{f}_1(t), \mathbf{f}_2(t), \mathbf{f}_3(t))$  can then be expressed [9] in terms of the ERF (5) and the polynomials  $a(t) = \operatorname{Re}(\mathbf{w}(t))$ ,  $b(t) = \operatorname{Im}(\mathbf{w}(t))$  as

$$\begin{aligned}\mathbf{f}_1(t) &= \mathbf{e}_1(t), \\ \mathbf{f}_2(t) &= \frac{a^2(t) - b^2(t)}{a^2(t) + b^2(t)} \mathbf{e}_2(t) - \frac{2a(t)b(t)}{a^2(t) + b^2(t)} \mathbf{e}_3(t), \\ \mathbf{f}_3(t) &= \frac{2a(t)b(t)}{a^2(t) + b^2(t)} \mathbf{e}_2(t) + \frac{a^2(t) - b^2(t)}{a^2(t) + b^2(t)} \mathbf{e}_3(t).\end{aligned}\quad (9)$$

This rational rotation-minimizing frame is of degree 8 in the curve parameter  $t$ .

### 3 Interpolation of $G^1$ spatial Hermite data

We are concerned with constructing quintic RRMF curves  $\mathbf{r}(t)$  for  $t \in [0, 1]$  that interpolate given  $G^1$  spatial Hermite data — i.e., initial/final points  $\mathbf{p}_i, \mathbf{p}_f$  and unit tangents  $\mathbf{t}_i, \mathbf{t}_f$ . Thus, the curve defined by (2)–(3) must satisfy (7)–(8) and

$$\mathbf{r}(0) = \mathbf{p}_i, \quad \frac{\mathbf{r}'(0)}{|\mathbf{r}'(0)|} = \mathbf{t}_i, \quad \mathbf{r}(1) = \mathbf{p}_f, \quad \frac{\mathbf{r}'(1)}{|\mathbf{r}'(1)|} = \mathbf{t}_f. \quad (10)$$

The unit tangents  $\mathbf{t}_i, \mathbf{t}_f$  can be specified in terms of polar angles  $\theta_i, \theta_f$  measured from the  $x$ -axis, and azimuthal angles  $\phi_i, \phi_f$  measured about the  $x$ -axis, as

$$\mathbf{t}_i = (\cos \theta_i, \sin \theta_i \cos \phi_i, \sin \theta_i \sin \phi_i), \quad (11)$$

$$\mathbf{t}_f = (\cos \theta_f, \sin \theta_f \cos \phi_f, \sin \theta_f \sin \phi_f). \quad (12)$$

Since the first condition in (10) is trivially satisfied by taking  $\mathbf{p}_i$  as integration constant on integrating (3), we need only consider the displacement

$$\Delta \mathbf{p} = \int_0^1 \mathbf{r}'(t) dt = \mathbf{p}_f - \mathbf{p}_i$$

rather than  $\mathbf{p}_i, \mathbf{p}_f$  individually. Now it is always possible to choose a coordinate system in which the initial tangent  $\mathbf{t}_i$  is in the  $(x, y)$ -plane, the initial point  $\mathbf{p}_i$  is at the origin, and the displacement  $\Delta \mathbf{p} = \mathbf{p}_f - \mathbf{p}_i$  lies on the  $x$ -axis. We say that such coordinates define *canonical Hermite data*, with  $\phi_i = 0$  and  $\Delta \mathbf{p} = (X, 0, 0)$ . We henceforth assume data of this form, and for brevity we write  $\phi_f = \phi$  and

$$(c_i, s_i) = (\cos \frac{1}{2}\theta_i, \sin \frac{1}{2}\theta_i), \quad (c_f, s_f) = (\cos \frac{1}{2}\theta_f, \sin \frac{1}{2}\theta_f). \quad (13)$$

Note that, for non-planar data,  $\theta_i, \theta_f$  and  $\phi$  must not be integer multiples of  $\pi$ .

Interpolation of the displacement  $\Delta \mathbf{p} = (X, 0, 0)$  by a PH quintic yields the two conditions

$$\begin{aligned} 5X &= |\alpha_0|^2 - |\beta_0|^2 \\ &+ \operatorname{Re}(\alpha_0 \bar{\alpha}_1 - \beta_0 \bar{\beta}_1) \\ &+ \frac{1}{3} \operatorname{Re}(\alpha_0 \bar{\alpha}_2 - \beta_0 \bar{\beta}_2) + \frac{2}{3} (|\alpha_1|^2 - |\beta_1|^2) \\ &+ \operatorname{Re}(\alpha_1 \bar{\alpha}_2 - \beta_1 \bar{\beta}_2) \\ &+ |\alpha_2|^2 - |\beta_2|^2, \end{aligned} \quad (14)$$

$$\begin{aligned} 0 &= 2\alpha_0 \bar{\beta}_0 \\ &+ \alpha_0 \bar{\beta}_1 + \alpha_1 \bar{\beta}_0 \\ &+ \frac{1}{3} (\alpha_0 \bar{\beta}_2 + \alpha_2 \bar{\beta}_0) + \frac{4}{3} \alpha_1 \bar{\beta}_1 \\ &+ \alpha_1 \bar{\beta}_2 + \alpha_2 \bar{\beta}_1 \\ &+ 2\alpha_2 \bar{\beta}_2. \end{aligned} \quad (15)$$

Since (14) is a scalar equation, while (15) is a relation among complex values, interpolating  $\Delta\mathbf{p}$  incurs *three* scalar constraints on the coefficients of  $\boldsymbol{\alpha}(t)$ ,  $\boldsymbol{\beta}(t)$ .

From (3) and (6), we can write the interpolation of end tangents as

$$\frac{\mathbf{r}'(0)}{|\mathbf{r}'(0)|} = \frac{(|\boldsymbol{\alpha}_0|^2 - |\boldsymbol{\beta}_0|^2, 2 \operatorname{Re}(\boldsymbol{\alpha}_0 \overline{\boldsymbol{\beta}_0}), 2 \operatorname{Im}(\boldsymbol{\alpha}_0 \overline{\boldsymbol{\beta}_0}))}{|\boldsymbol{\alpha}_0|^2 + |\boldsymbol{\beta}_0|^2} = \mathbf{t}_i, \quad (16)$$

$$\frac{\mathbf{r}'(1)}{|\mathbf{r}'(1)|} = \frac{(|\boldsymbol{\alpha}_2|^2 - |\boldsymbol{\beta}_2|^2, 2 \operatorname{Re}(\boldsymbol{\alpha}_2 \overline{\boldsymbol{\beta}_2}), 2 \operatorname{Im}(\boldsymbol{\alpha}_2 \overline{\boldsymbol{\beta}_2}))}{|\boldsymbol{\alpha}_2|^2 + |\boldsymbol{\beta}_2|^2} = \mathbf{t}_f. \quad (17)$$

Since  $\mathbf{t}_i$  and  $\mathbf{t}_f$  are *unit* vectors, (16) and (17) each yield two scalar constraints on the coefficients of  $\boldsymbol{\alpha}(t)$ ,  $\boldsymbol{\beta}(t)$ . Hence, the  $G^1$  Hermite interpolation conditions impose *seven* scalar constraints on the *six* complex coefficients of the polynomials  $\boldsymbol{\alpha}(t)$  and  $\boldsymbol{\beta}(t)$ . Thus, in conjunction with the RRMF constraints (7)–(8), we have altogether *ten* scalar constraints and *twelve* scalar unknowns.

Another scalar constraint may be imposed by noting [10] that the polynomials (6) embody one non-essential freedom. Namely, if  $\boldsymbol{\alpha}(t)$ ,  $\boldsymbol{\beta}(t)$  generate a specific hodograph  $\mathbf{r}'(t)$  through (3), the same hodograph is obtained on replacing them by  $\exp(i\xi)\boldsymbol{\alpha}(t)$ ,  $\exp(i\xi)\boldsymbol{\beta}(t)$  for any  $\xi \in \mathbb{R}$ . Hence we may assume, without loss of generality, that one of the coefficients in (6) is *real*. Thus, we expect the RRMF quintic interpolants to given spatial  $G^1$  Hermite data to form a one-parameter family of space curves.

## 4 Solution of RRMF Hermite system

As noted in Sections 2 and 3, the interpolation of  $G^1$  Hermite data by RRMF quintic curves involves a system of eleven scalar constraints on the six complex coefficients  $\boldsymbol{\alpha}_0, \boldsymbol{\alpha}_1, \boldsymbol{\alpha}_2, \boldsymbol{\beta}_0, \boldsymbol{\beta}_1, \boldsymbol{\beta}_2$ , leaving one scalar degree of freedom. Consider first interpolation of the end tangents.

**Proposition 1** *For canonical-form Hermite data, interpolation of the two end tangents (11)–(12) may be achieved by expressing  $\boldsymbol{\alpha}_0, \boldsymbol{\beta}_0$  and  $\boldsymbol{\alpha}_2, \boldsymbol{\beta}_2$  in terms of complex values  $\gamma_0$  and  $\gamma_2$  as*

$$\boldsymbol{\alpha}_0 = \gamma_0 c_i, \quad \boldsymbol{\alpha}_2 = \gamma_2 c_f \exp(i\frac{1}{2}\phi), \quad (18)$$

$$\boldsymbol{\beta}_0 = \gamma_0 s_i, \quad \boldsymbol{\beta}_2 = \gamma_2 s_f \exp(-i\frac{1}{2}\phi). \quad (19)$$

**Proof :** Substituting (18)–(19) in (16)–(17) and simplifying yields (11)–(12). ■

From (18) and (19) we see that

$$|\boldsymbol{\alpha}_0|^2 + |\boldsymbol{\beta}_0|^2 = |\gamma_0|^2 \quad \text{and} \quad |\boldsymbol{\alpha}_2|^2 + |\boldsymbol{\beta}_2|^2 = |\gamma_2|^2.$$

Thus, denoting by  $\rho^2$  the ratio of the end-derivative magnitudes,

$$\rho^2 = \frac{|\mathbf{r}'(1)|}{|\mathbf{r}'(0)|} = \frac{|\boldsymbol{\alpha}_2|^2 + |\boldsymbol{\beta}_2|^2}{|\boldsymbol{\alpha}_0|^2 + |\boldsymbol{\beta}_0|^2}, \quad (20)$$

we have

$$|\gamma_2| = \rho |\gamma_0|.$$

Therefore, we can write  $\gamma_0 = \gamma \exp(i\lambda_0)$  and  $\gamma_2 = \rho \gamma \exp(i\lambda_2)$  where  $\gamma, \rho \in \mathbb{R}^+$  and  $\lambda_0, \lambda_2 \in [0, 2\pi]$ . The redundancy of the representation (2) can be used to fix either  $\lambda_0$  or  $\lambda_2$ . We choose  $\lambda_0 = 0$  and, for simplicity, set  $\lambda_2 = \lambda$ . Invoking the notations (13), we obtain the expressions

$$\alpha_0 = \gamma c_i, \quad \alpha_2 = \rho \gamma c_f \exp(i(\lambda + \frac{1}{2}\phi)), \quad (21)$$

$$\beta_0 = \gamma s_i, \quad \beta_2 = \rho \gamma s_f \exp(i(\lambda - \frac{1}{2}\phi)), \quad (22)$$

where  $c_i, s_i, c_f, s_f \neq 0$  and  $\phi$  is not an integer multiple of  $\pi$  for non-planar data.

Consider now the RRMF conditions (7)–(8). Substituting the expressions for  $\alpha_0, \beta_0, \alpha_2, \beta_2$  and simplifying yields

$$|c_f \exp(i\frac{1}{2}\phi) \bar{\alpha}_1 + s_f \exp(-i\frac{1}{2}\phi) \bar{\beta}_1| = |c_i \bar{\alpha}_1 + s_i \bar{\beta}_1|, \quad (23)$$

$$\begin{aligned} \rho \gamma^2 \exp(i\lambda) [c_i s_f \exp(-i\frac{1}{2}\phi) - c_f s_i \exp(i\frac{1}{2}\phi)] \\ = 2(c_i \bar{\alpha}_1 + s_i \bar{\beta}_1)(c_i \beta_1 - s_i \alpha_1). \end{aligned} \quad (24)$$

Condition (23) implies that, for some angular parameter  $\eta$ , we must have

$$\exp(i\eta) [c_f \exp(i\frac{1}{2}\phi) \bar{\alpha}_1 + s_f \exp(-i\frac{1}{2}\phi) \bar{\beta}_1] = c_i \bar{\alpha}_1 + s_i \bar{\beta}_1,$$

and hence

$$[s_f \exp(i\frac{1}{2}\phi) - s_i \exp(i\eta)] \beta_1 = [c_i \exp(i\eta) - c_f \exp(-i\frac{1}{2}\phi)] \alpha_1. \quad (25)$$

Now if  $\eta$  is such that  $s_f \exp(i\frac{1}{2}\phi) = s_i \exp(i\eta)$ , condition (25) implies that  $\alpha_1 = 0$ . This is possible only if  $s_f = s_i$  and  $\eta = \frac{1}{2}\phi$ , or  $s_f = -s_i$  and  $\eta = \frac{1}{2}\phi + \pi$ . In the former case (24) is satisfied by taking  $\lambda = \frac{1}{2}\pi$  or  $\frac{3}{2}\pi$  and  $|\beta_1|^2 = \rho \gamma^2 |\sin \frac{1}{2}\phi|$ . In the latter case (24) is satisfied with  $\lambda = 0$  or  $\pi$  and  $|\beta_1|^2 = \rho \gamma^2 |\cos \frac{1}{2}\phi|$ . In all other cases (25) implies that

$$\beta_1 = \frac{c_i \exp(i\eta) - c_f \exp(-i\frac{1}{2}\phi)}{s_f \exp(i\frac{1}{2}\phi) - s_i \exp(i\eta)} \alpha_1. \quad (26)$$

Substituting (26) into (24), cancelling the factor<sup>4</sup>  $c_i s_f \exp(-i\frac{1}{2}\phi) - c_f s_i \exp(i\frac{1}{2}\phi)$  from both sides, and setting  $\epsilon = c_i c_f \exp(-i\frac{1}{2}\phi) + s_i s_f \exp(i\frac{1}{2}\phi)$ , we obtain

$$|\alpha_1|^2 = \frac{1}{2} \rho \gamma^2 \frac{|s_f \exp(i\frac{1}{2}\phi) - s_i \exp(i\eta)|^2}{\exp(-i\lambda) [\exp(i\eta) - \epsilon]}. \quad (27)$$

For a valid solution, the expression on the right must have a non-negative real value. This is equivalent to satisfaction of the relations

$$\text{Im}(\exp(-i\lambda) [\exp(i\eta) - \epsilon]) = 0, \quad \text{Re}(\exp(-i\lambda) [\exp(i\eta) - \epsilon]) > 0,$$

<sup>4</sup> Under the stated assumptions on  $c_i, s_i, c_f, s_f$  and  $\phi$ , this factor is always non-zero. The same is true of the term  $\exp(i\eta) - \epsilon$ , for all values of  $\eta$ .

by the parameters  $\eta$  and  $\lambda$ , and consequently

$$\exp(-i\lambda) = \boldsymbol{\mu}_0(\eta) \quad \text{with} \quad \boldsymbol{\mu}_0(\eta) = \frac{\exp(-i\eta) - \bar{\boldsymbol{\epsilon}}}{|\exp(-i\eta) - \bar{\boldsymbol{\epsilon}}|}. \quad (28)$$

Substituting from (28) into (27), we obtain

$$|\boldsymbol{\alpha}_1|^2 = \rho \gamma^2 f_1(\eta) \quad \text{with} \quad f_1(\eta) = \frac{\frac{1}{2} |s_f \exp(i\frac{1}{2}\phi) - s_i \exp(i\eta)|^2}{|\exp(i\eta) - \boldsymbol{\epsilon}|}. \quad (29)$$

Assuming that<sup>5</sup>  $3\bar{\boldsymbol{\alpha}}_0 + 4\bar{\boldsymbol{\alpha}}_1 + 3\bar{\boldsymbol{\alpha}}_2 \neq 0$ , equation (15) allows  $\boldsymbol{\beta}_1$  to be expressed in terms of  $\boldsymbol{\alpha}_1$  as

$$\boldsymbol{\beta}_1 = - \frac{(6\beta_0 + \beta_2)\bar{\boldsymbol{\alpha}}_0 + 3(\beta_0 + \beta_2)\bar{\boldsymbol{\alpha}}_1 + (\beta_0 + 6\beta_2)\bar{\boldsymbol{\alpha}}_2}{3\bar{\boldsymbol{\alpha}}_0 + 4\bar{\boldsymbol{\alpha}}_1 + 3\bar{\boldsymbol{\alpha}}_2}.$$

Equating this expression for  $\boldsymbol{\beta}_1$  with (26) and cancelling  $\gamma$  from both sides gives the equation

$$\boldsymbol{\delta}_0(\eta, \rho) \boldsymbol{\alpha}_1 + \boldsymbol{\delta}_1(\eta, \rho) \bar{\boldsymbol{\alpha}}_1 = \gamma \boldsymbol{\delta}_2(\eta, \rho), \quad (30)$$

for  $\boldsymbol{\alpha}_1$ , with coefficients

$$\begin{aligned} \boldsymbol{\delta}_0(\eta, \rho) &= 3 [c_i + \rho c_f \boldsymbol{\mu}_0 \exp(-i\frac{1}{2}\phi)] \boldsymbol{\mu}_1, \\ \boldsymbol{\delta}_1(\eta, \rho) &= 3 [s_i + \rho s_f \bar{\boldsymbol{\mu}}_0 \exp(-i\frac{1}{2}\phi)], \\ \boldsymbol{\delta}_2(\eta, \rho) &= -6 [c_i s_i + \rho^2 c_f s_f \exp(-i\phi)] - 4\rho f_1 \boldsymbol{\mu}_1 \\ &\quad - \rho \exp(-i\frac{1}{2}\phi) [c_i s_f \bar{\boldsymbol{\mu}}_0 + c_f s_i \boldsymbol{\mu}_0], \end{aligned} \quad (31)$$

where we define

$$\boldsymbol{\mu}_1(\eta) = \frac{c_i \exp(i\eta) - c_f \exp(-i\frac{1}{2}\phi)}{s_f \exp(i\frac{1}{2}\phi) - s_i \exp(i\eta)}. \quad (32)$$

Now the pairs of  $(\rho, \eta)$  values such that  $|\boldsymbol{\delta}_0|^2 = |\boldsymbol{\delta}_1|^2$  and  $\text{Re}((\boldsymbol{\delta}_0 - \boldsymbol{\delta}_1)\bar{\boldsymbol{\delta}}_2) \neq 0$  or  $\text{Im}((\boldsymbol{\delta}_0 + \boldsymbol{\delta}_1)\bar{\boldsymbol{\delta}}_2) \neq 0$  are unacceptable, because equation (30) has no solution. On the other hand, if there exist pairs such that  $|\boldsymbol{\delta}_0|^2 = |\boldsymbol{\delta}_1|^2$  and  $\text{Re}((\boldsymbol{\delta}_0 - \boldsymbol{\delta}_1)\bar{\boldsymbol{\delta}}_2) = \text{Im}((\boldsymbol{\delta}_0 + \boldsymbol{\delta}_1)\bar{\boldsymbol{\delta}}_2) = 0$ , equation (30) corresponds to only one scalar condition. In this special case, we also need equation (29) to determine  $\boldsymbol{\alpha}_1$ .

In general, we can assume that  $|\boldsymbol{\delta}_0|^2 \neq |\boldsymbol{\delta}_1|^2$  and derive  $\boldsymbol{\alpha}_1$  from (30) as

$$\boldsymbol{\alpha}_1 = \gamma \frac{\bar{\boldsymbol{\delta}}_0 \boldsymbol{\delta}_2 - \boldsymbol{\delta}_1 \bar{\boldsymbol{\delta}}_2}{|\boldsymbol{\delta}_0|^2 - |\boldsymbol{\delta}_1|^2}.$$

Once  $\eta$  is chosen, the correct  $\rho$  value is identified via (29) by the positive real roots of the equation

$$|\bar{\boldsymbol{\delta}}_0 \boldsymbol{\delta}_2 - \boldsymbol{\delta}_1 \bar{\boldsymbol{\delta}}_2|^2 - \rho f_1(\eta) (|\boldsymbol{\delta}_0|^2 - |\boldsymbol{\delta}_1|^2)^2 = 0, \quad (33)$$

<sup>5</sup> This incurs no loss of generality: the condition  $\boldsymbol{\alpha}_1 = -\frac{3}{4}(\boldsymbol{\alpha}_0 + \boldsymbol{\alpha}_2)$  imposes two more scalar constraints on  $\eta$  and  $\rho$ , so no degrees of freedom remain for satisfying (27).

which is a polynomial equation of degree 6 with real coefficients. We may write

$$\bar{\delta}_0 \delta_2 - \delta_1 \bar{\delta}_2 = \sum_{k=0}^3 \mathbf{z}_k \rho^k,$$

with

$$\begin{aligned} \mathbf{z}_0 &= 18 c_i s_i (s_i - c_i \bar{\mu}_1), \\ \mathbf{z}_1 &= 18 c_i s_i \bar{\mu}_0 [s_f \exp(-i\frac{1}{2}\phi) - c_f \bar{\mu}_1 \exp(i\frac{1}{2}\phi)] + 3 s_i \exp(i\frac{1}{2}\phi) (c_i s_f \mu_0 + c_f s_i \bar{\mu}_0) \\ &\quad + 12 f_1 \bar{\mu}_1 (s_i - c_i \mu_1) - 3 c_i \bar{\mu}_1 \exp(-i\frac{1}{2}\phi) (c_i s_f \bar{\mu}_0 + c_f s_i \mu_0), \\ \mathbf{z}_2 &= 18 c_f s_f [s_i \exp(i\phi) - c_i \bar{\mu}_1 \exp(-i\phi)] + 3 s_f \bar{\mu}_0 (c_i s_f \mu_0 + c_f s_i \bar{\mu}_0) \\ &\quad + 12 f_1 \bar{\mu}_0 \bar{\mu}_1 [s_f \exp(-i\frac{1}{2}\phi) - c_f \mu_1 \exp(i\frac{1}{2}\phi)] - 3 c_f \bar{\mu}_1 \bar{\mu}_0 (c_i s_f \bar{\mu}_0 + c_f s_i \mu_0), \\ \mathbf{z}_3 &= 18 c_f s_f \bar{\mu}_0 [s_f \exp(i\frac{1}{2}\phi) - c_f \bar{\mu}_1 \exp(-i\frac{1}{2}\phi)], \end{aligned}$$

while

$$|\delta_0|^2 = \sum_{k=0}^2 d_{0k} \rho^k \quad \text{and} \quad |\delta_1|^2 = \sum_{k=0}^2 d_{1k} \rho^k,$$

with

$$\begin{aligned} d_{00} &= 9 |\mu_1|^2 c_i^2, \\ d_{01} &= 9 |\mu_1|^2 c_i c_f [\mu_0 \exp(-i\frac{1}{2}\phi) + \bar{\mu}_0 \exp(i\frac{1}{2}\phi)], \\ d_{02} &= 9 |\mu_1|^2 |\mu_0|^2 c_f^2, \\ d_{10} &= 9 s_i^2, \\ d_{11} &= 9 s_i s_f [\bar{\mu}_0 \exp(-i\frac{1}{2}\phi) + \mu_0 \exp(i\frac{1}{2}\phi)], \\ d_{12} &= 9 |\mu_0|^2 s_f^2. \end{aligned}$$

Hence, setting

$$|\bar{\delta}_0 \delta_2 - \delta_1 \bar{\delta}_2|^2 = \sum_{k=0}^6 c_k \rho^k,$$

where

$$\begin{aligned} c_0 &= |\mathbf{z}_0|^2, \\ c_1 &= 2 \operatorname{Re}(\mathbf{z}_1 \bar{\mathbf{z}}_0), \\ c_2 &= 2 \operatorname{Re}(\mathbf{z}_2 \bar{\mathbf{z}}_0) + |\mathbf{z}_1|^2, \\ c_3 &= 2 \operatorname{Re}(\mathbf{z}_3 \bar{\mathbf{z}}_0) + 2 \operatorname{Re}(\mathbf{z}_2 \bar{\mathbf{z}}_1), \\ c_4 &= 2 \operatorname{Re}(\mathbf{z}_3 \bar{\mathbf{z}}_1) + |\mathbf{z}_2|^2, \\ c_5 &= 2 \operatorname{Re}(\mathbf{z}_3 \bar{\mathbf{z}}_2), \\ c_6 &= |\mathbf{z}_3|^2, \end{aligned} \tag{34}$$

equation (33) reduces to

$$c_6 \rho^6 + \sum_{j=1}^5 (c_j - e_{j-1} f_1) \rho^j + c_0 = 0, \quad (35)$$

with

$$\begin{aligned} e_0 &= (d_{00} - d_{10})^2, \\ e_1 &= 2(d_{00} - d_{10})(d_{01} - d_{11}), \\ e_2 &= (d_{01} - d_{11})^2 + 2(d_{00} - d_{10})(d_{02} - d_{12}), \\ e_3 &= 2(d_{01} - d_{11})(d_{02} - d_{12}), \\ e_4 &= (d_{02} - d_{12})^2. \end{aligned}$$

Equation (35) must possess at least one positive real root, for some value of the angular parameter  $\eta$ , if an RRMF quintic  $G^1$  Hermite interpolant is to exist. Since the coefficients of (35) have a complicated, non-linear dependence on the Hermite data and on the parameter  $\eta$ , a thorough investigation of the existence (and number) of interpolants is a challenging task, beyond our present scope. We hope to address it in a future study.

From (21)–(22) and (26)–(27) we observe that the coefficients of  $\alpha(t)$ ,  $\beta(t)$  are all proportional to  $\gamma$ . Hence, we may write

$$\alpha_k = \gamma \mathbf{a}_k \quad \text{and} \quad \beta_k = \gamma \mathbf{b}_k \quad (36)$$

for  $k = 0, 1, 2$ , where

$$\mathbf{a}_0 = c_i, \quad \mathbf{a}_1 = \frac{\bar{\delta}_0 \delta_2 - \delta_1 \bar{\delta}_2}{|\delta_0|^2 - |\delta_1|^2}, \quad \mathbf{a}_2 = \rho c_f \bar{\mu}_0 \exp(i\frac{1}{2}\phi), \quad (37)$$

$$\mathbf{b}_0 = s_i, \quad \mathbf{b}_1 = \mu_1 \mathbf{a}_1, \quad \mathbf{b}_2 = \rho s_f \bar{\mu}_0 \exp(-i\frac{1}{2}\phi). \quad (38)$$

Substituting (36) into (14), the  $\gamma$  value corresponding to a positive real root of (35) can be computed as

$$\gamma = \sqrt{\frac{5X}{f_2(\eta)}}, \quad (39)$$

where  $f_2(\eta)$  is defined by

$$\begin{aligned} f_2(\eta) &= |\mathbf{a}_0|^2 - |\mathbf{b}_0|^2 + \operatorname{Re}(\mathbf{a}_0 \bar{\mathbf{a}}_1 - \mathbf{b}_0 \bar{\mathbf{b}}_1) \\ &\quad + \frac{1}{3} \operatorname{Re}(\mathbf{a}_0 \bar{\mathbf{a}}_2 - \mathbf{b}_0 \bar{\mathbf{b}}_2) + \frac{2}{3} (|\mathbf{a}_1|^2 - |\mathbf{b}_1|^2) \\ &\quad + \operatorname{Re}(\mathbf{a}_1 \bar{\mathbf{a}}_2 - \mathbf{b}_1 \bar{\mathbf{b}}_2) + |\mathbf{a}_2|^2 - |\mathbf{b}_2|^2. \end{aligned} \quad (40)$$

Of course, we must require  $f_2(\eta) > 0$  for (39) to yield a real  $\gamma$  value. Again, due to the complicated dependence of (40) on  $\eta$  and the prescribed Hermite data, a detailed study of the conditions under which this holds is deferred to a future study. For the present, we only observe from experience with experimental tests

that there are infinitely many admissible choices for  $\eta$  in the case of sufficiently dense data sampled from a smooth analytic curve, some of which produce very reasonable shapes. On the other hand, as shown in the examples of the following section, we have also been able to identify admissible fair-shaped RRMF quintic interpolants for many other data sets.

We conclude by summarizing the computation of RRMF quintic interpolants to spatial  $G^1$  Hermite data as follows (for brevity, we exclude the cases  $\eta = \frac{1}{2}\phi$  when  $s_f = s_i$ , and  $\eta = \frac{1}{2}\phi + \pi$  when  $s_f = -s_i$ ). The procedure employs  $N_\eta$  uniformly-sampled values of the  $\eta$  parameter.

### Algorithm

Input:  $\mathbf{p}_i, \mathbf{p}_f, \mathbf{t}_i, \mathbf{t}_f, N_\eta$

1. transform the Hermite data to canonical form;
2. determine  $\theta_i, \theta_f, \phi = \phi_f$  from expressions (11)–(12);
3. compute  $c_i, s_i$  and  $c_f, s_f$  from (13);
4. compute  $\epsilon = c_i c_f \exp(-i\frac{1}{2}\phi) + s_i s_f \exp(i\frac{1}{2}\phi)$ ;
5. for  $\eta = 2\pi k/N_\eta$  with  $k = 0, \dots, N_\eta - 1$ :
  - (a) compute  $\mu_0, \mu_1, f_1$  from (28), (32), (29);
  - (b) compute  $c_0, \dots, c_6$  from (34);
  - (c) find a positive real root  $\rho$  of equation (35);  
if no positive real root exists, return to step 5;
  - (d) compute  $\delta_0, \delta_1, \delta_2$  from (31);
  - (e) compute  $\mathbf{a}_0, \mathbf{a}_1, \mathbf{a}_2$  and  $\mathbf{b}_0, \mathbf{b}_1, \mathbf{b}_2$  from (37) and (38);
  - (f) compute  $f_2$  from (40) — if  $f_2 \leq 0$  return to step 5;
  - (g) determine  $\gamma$  from expression (39);
  - (h) compute  $\alpha_0, \alpha_1, \alpha_2$  and  $\beta_0, \beta_1, \beta_2$  from (36)–(38);
  - (i) construct the hodograph (2) from  $\alpha(t)$  and  $\beta(t)$ ;
  - (j) transform to original coordinates by inverting step 1.

Output: a set of RRMF quintics interpolating the Hermite data, corresponding to the chosen  $\eta$  values.

## 5 Numerical results

The numerical results show that the  $\eta, \rho$  values can significantly influence the shape of the resulting RRMF interpolant. In computing the following examples, we used the MATLAB function `roots` to solve (35). The Bernstein coefficients of the polynomials  $\alpha(t), \beta(t), \mathbf{w}(t)$  are quoted to five significant digits.

**Example 1** Figure 1 shows two RRMF quintic interpolants to the data

$$\mathbf{p}_0 = (0, 0, 0), \quad \mathbf{p}_1 = (1, 1, 1), \quad \mathbf{t}_0 = \frac{(1, 0, 1)}{\sqrt{2}}, \quad \mathbf{t}_1 = \frac{(0, 1, 1)}{\sqrt{2}},$$

together with their Bézier control polygons. After transforming this data to canonical form, the coefficients of the  $\alpha(t)$ ,  $\beta(t)$ ,  $\mathbf{w}(t)$  polynomials are

$$\begin{aligned} \alpha_0 &= 1.4194, & \alpha_1 &= -0.7920 + 0.4058i, & \alpha_2 &= -0.9158 + 2.5605i, \\ \beta_0 &= 0.4512, & \beta_1 &= 1.1392 + 0.7361i, & \beta_2 &= -0.5593 - 0.6590i, \\ \mathbf{w}_0 &= 1.0, & \mathbf{w}_1 &= -0.2751 + 0.4094i, & \mathbf{w}_2 &= 1.1863 + 1.5044i, \end{aligned}$$

for the curve on the left with  $(\eta, \rho) = (5.2000, 1.9158)$ , and

$$\begin{aligned} \alpha_0 &= 1.5363, & \alpha_1 &= 1.1372 + 0.4334i, & \alpha_2 &= 0.7595 + 1.2735i, \\ \beta_0 &= 0.4883, & \beta_1 &= -0.0461 - 0.2865i, & \beta_2 &= -0.4712 + 0.0067i, \\ \mathbf{w}_0 &= 1.0, & \mathbf{w}_1 &= 0.6637 + 0.2024i, & \mathbf{w}_2 &= 0.6024 + 0.7542i, \end{aligned}$$

for the curve on the right with  $(\eta, \rho) = (4.3250, 0.9652)$ . Both cases satisfy (4).

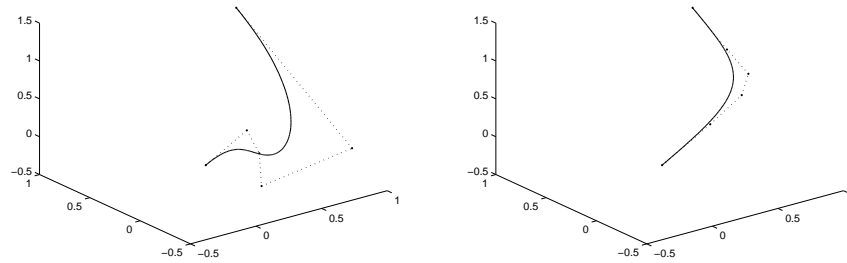


**Fig. 1.** The RRMF quintic interpolants of Example 1, with Bézier control polygons.

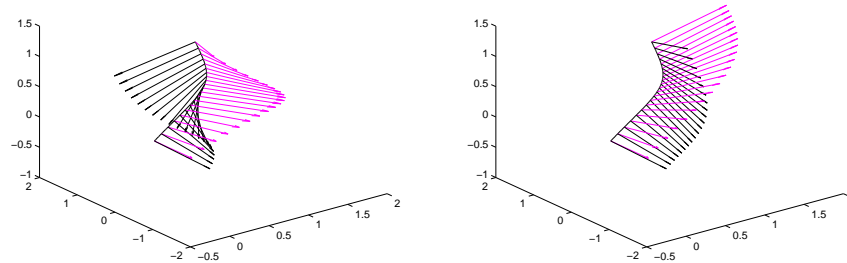


**Fig. 2.** Comparison of the ERF (left) and RMF (right) along the RRMF quintic shown on the right in Figure 1. For clarity, the unit tangent vector is omitted from the plots.

The corresponding values of the shape integrals<sup>6</sup> (89) in [8] are

$$L = 2.3259, \quad E = 44.509, \quad E_{\text{rmf}} = 22.856,$$

for the curve on the left, and

$$L = 1.9070, \quad E = 5.7495, \quad E_{\text{rmf}} = 1.4641,$$

for the curve on the right. Figure 2 shows the variation of the ERF and RMF along the RRMF quintic on the right in Figure 1.

**Example 2** Figure 3 shows two RRMF quintic interpolants to the data

$$\mathbf{p}_0 = (0, 0, 0), \quad \mathbf{p}_1 = (1, 0, 0), \quad \mathbf{t}_0 = \frac{(1, 1, 0)}{\sqrt{2}}, \quad \mathbf{t}_1 = \frac{\mathbf{d}_1}{|\mathbf{d}_1|},$$

where  $\mathbf{d}_1 = (0.2, 0.2, 0.4057)$ , together with their Bézier control polygons. In this case, the coefficients of the  $\boldsymbol{\alpha}(t)$ ,  $\boldsymbol{\beta}(t)$ ,  $\mathbf{w}(t)$  polynomials are

$$\begin{aligned} \boldsymbol{\alpha}_0 &= 1.9240, & \boldsymbol{\alpha}_1 &= 0.3403 - 0.9857i, & \boldsymbol{\alpha}_2 &= -0.8882 - 1.2811i, \\ \boldsymbol{\beta}_0 &= 0.7970, & \boldsymbol{\beta}_1 &= 0.1805 + 1.4013i, & \boldsymbol{\beta}_2 &= -1.0041 + 0.1499i, \\ \mathbf{w}_0 &= 1.0, & \mathbf{w}_1 &= 0.1841 - 0.1798i, & \mathbf{w}_2 &= 0.7110 - 0.5408i, \end{aligned}$$

for the curve on the left with  $(\eta, \rho) = (4.2000, 0.8933)$ , and

$$\begin{aligned} \boldsymbol{\alpha}_0 &= 2.0292, & \boldsymbol{\alpha}_1 &= 0.8559 - 0.4150i, & \boldsymbol{\alpha}_2 &= -0.7008 - 1.0107i, \\ \boldsymbol{\beta}_0 &= 0.8405, & \boldsymbol{\beta}_1 &= -0.7890 + 1.0190i, & \boldsymbol{\beta}_2 &= -0.7921 + 0.1183i, \\ \mathbf{w}_0 &= 1.0, & \mathbf{w}_1 &= 0.2226 + 0.0030i, & \mathbf{w}_2 &= 0.5319 - 0.4045i, \end{aligned}$$

for the curve on the right with  $(\eta, \rho) = (4.2000, 0.6682)$ . Both curves satisfy (4). The values of the shape integrals are

$$L = 2.1610, \quad E = 15.806, \quad E_{\text{rmf}} = 12.807$$

for the curve on the left, and

$$L = 1.9263, \quad E = 19.945, \quad E_{\text{rmf}} = 15.998,$$

for the curve on the right. Figure 4 shows the variation of the ERF and RMF along the RRMF quintic on the left in Figure 3.

**Example 3** In the final example, we consider data obtained by sampling the circular helix  $\mathbf{r}(t) = (\sin(t), \cos(t), t)$  at ten equidistant points on  $t \in [0, \frac{9}{2}\pi]$ . The resulting  $G^1$  RRMF quintic interpolants are illustrated in Figure 5.

<sup>6</sup>  $L$  is the total arc length;  $E$  is the elastic energy associated with the Frenet frame; and  $E_{\text{rmf}}$  is the energy associated with the RMF.

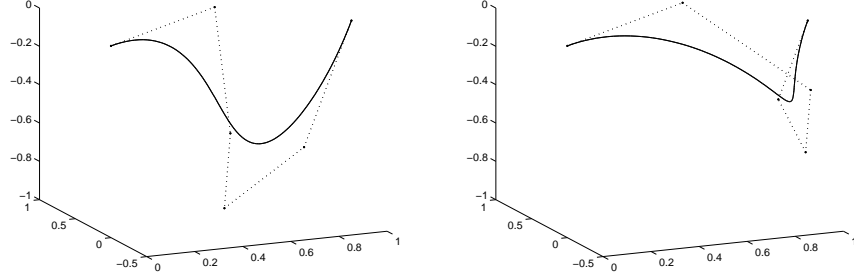


**Fig. 3.** The RRMF quintic interpolants of Example 2, with Bézier control polygons.

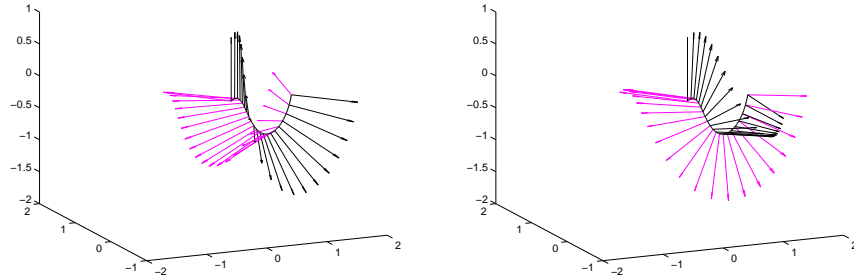


**Fig. 4.** Comparison of the ERF (left) and RMF (right) along the RRMF quintic shown on the left in Figure 3. For clarity, the unit tangent vector is omitted in these plots.

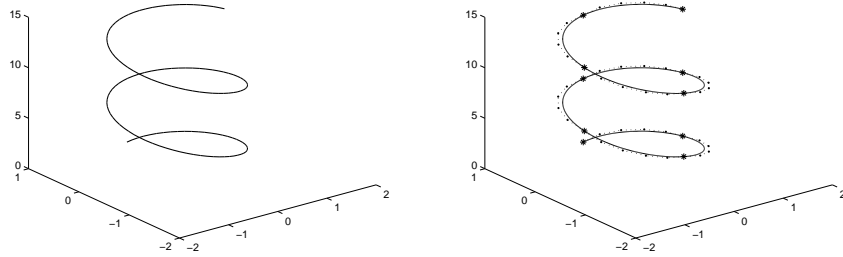


**Fig. 5.** A piecewise  $G^1$  RRMF quintic interpolant (right) to Hermite data sampled from the circular helix (left). For each spline segment (delimited by the \* symbols) the RRMF quintic Hermite interpolant is shown together with its Bézier control polygon.

## 6 Closure

A method for computing quintic RRMF (rational rotation–minimizing frame) curves that interpolate spatial  $G^1$  Hermite data has been presented. Such curves are useful in applications such as motion control, animation, and swept surface constructions. The method involves one free angular parameter, that can strongly influence the curve shape. Numerical experiments show that, for many Hermite data sets, interpolants of good shape can be obtained by the method, but the formulation of an automatic and efficient procedure for their selection is an open problem. Further open problems concern the existence and multiplicity of the interpolants to arbitrary Hermite data, and the geometrical significance of the parameter  $\eta$ . Because they are highly non–linear, these problems are non–trivial: we hope to address them more carefully in future studies.

## References

1. R. L. Bishop (1975), There is more than one way to frame a curve, *American Mathematical Monthly* **82**, 246–251.
2. H. I. Choi and C. Y. Han (2002), Euler–Rodrigues frames on spatial Pythagorean–hodograph curves, *Computer Aided Geometric Design* **19**, 603–620.
3. H. I. Choi, D. S. Lee, and H. P. Moon (2002), Clifford algebra, spin representation, and rational parameterization of curves and surfaces, *Advances in Computational Mathematics* **17**, 5–48.
4. R. T. Farouki (2002), Exact rotation–minimizing frames for spatial Pythagorean–hodograph curves, *Graphical Models* **64**, 382–395.
5. R. T. Farouki (2008), *Pythagorean–Hodograph Curves: Algebra and Geometry Inseparable*, Springer, Berlin.
6. R. T. Farouki, M. al–Kandari, and T. Sakkalis (2002), Hermite interpolation by rotation–invariant spatial Pythagorean–hodograph curves, *Advances in Computational Mathematics* **17**, 369–383.
7. R. T. Farouki and C. Giannelli (2008), Spatial camera orientation control by rotation–minimizing directed frames, *Computer Animation and Virtual Worlds* to appear.
8. R. T. Farouki, C. Giannelli, C. Manni, and A. Sestini (2008), Identification of spatial PH quintic Hermite interpolants with near–optimal shape measures, *Computer Aided Geometric Design* **25**, 274–297.
9. R. T. Farouki, C. Giannelli, C. Manni, and A. Sestini (2009), Quintic space curves with rational rotation–minimizing frames, *Computer Aided Geometric Design* to appear.
10. R. T. Farouki, C. Giannelli, and A. Sestini (2009), Helical polynomial curves and double Pythagorean hodographs I. Quaternion and Hopf map representation, *Journal of Symbolic Computation* **44**, 161–179.
11. R. T. Farouki and C. Y. Han (2003), Rational approximation schemes for rotation–minimizing frames on Pythagorean–hodograph curves, *Computer Aided Geometric Design* **20**, 435–454.
12. H. Guggenheimer (1989), Computing frames along a trajectory, *Computer Aided Geometric Design* **6**, 77–78.

13. C. Y. Han (2008), Nonexistence of rational rotation-minimizing frames on cubic curves, *Computer Aided Geometric Design* **25**, 298–304.
14. B. Jüttler, C. Mäurer (1999), Cubic Pythagorean hodograph spline curves and applications to sweep surface modeling, *Computer Aided Design* **31**, 73–83.
15. F. Klok (1986), Two moving coordinate frames for sweeping along a 3D trajectory, *Computer Aided Geometric Design* **3**, 217–229.
16. Z. Sir and B. Jüttler (2005), Spatial Pythagorean hodograph quintics and the approximation of pipe surfaces, in *Mathematics of Surfaces XI* (R. Martin, H. Bez, and M. Sabin, eds.) Springer, Berlin, pp. 364–380.
17. W. Wang and B. Joe (1997), Robust computation of the rotation minimizing frame for sweep surface modelling, *Computer Aided Design* **29**, 379–391.
18. W. Wang, B. Jüttler, D. Zheng, Y. Liu (2008), Computation of rotation minimizing frames. *ACM Transactions on Graphics* **27**, No. 1, Article 2, 1–18.